Supplementary Information for "A Case Study into the Measurement of Ship Emissions from Plume Intercepts of the NOAA Ship Miller Freeman"

C. D. Cappa[1,*], E. J. Williams[2,3], D. A. Lack[2,3], G. M. Buffaloe[1], D. Coffman[7], K. L. Hayden[5], S. C. Herndon[4], B. M. Lerner[2,3], S-M. Li[5], P. Massoli[4], R. McLaren[6], I. Nuaaman,[5,6] T. B. Onasch[4], P. K. Quinn[7]

[1] {Department of Civil and Environmental Engineering, University of California, Davis, California 95616, USA}

[2] {NOAA Earth System Research Laboratory, Boulder, CO, 80305, USA}

[3] {Cooperative Institute for Research in Environmental Sciences, University of Colorado, Boulder, Colorado, 80305, USA}

[4] {Aerodyne Research, Inc., Billerica, Massachusetts, USA, 01821}

[5] {Air Quality Research Division, Environment Canada, 4905 Dufferin St., Toronto, Canada, M3H5T4}

[6] {Centre for Atmospheric Chemistry, York University, 4700 Keele St., Toronto, Canada, M3J1P3}

[7] {NOAA Pacific Marine Environment Laboratory, Seattle, Washington, 98115, USA}

Correspondence to: C. D. Cappa (cdcappa@ucdavis.edu)

Overview

The Supplementary Information provides: (i) a table with information about the engine/ship type for the literature studies; (ii) information on the conversion between mass-based and energy-based emission factors (EFs); (iii) information on the determination of the SP-AMS collection efficiency; (iv) information operation of the CCN instrument, and; (v) further details about the SP2 data processing.

1. Absolute Values of the BC and EC Emission Factors

Table S1 provides information on the engine type, ship type and fuel used in the various literature studies discussed in the main text.

2. Conversion of Literature Black Carbon (BC) and Elemental Carbon (EC) Emission Factors

Many of the literature studies report the EF_{BC} values in units of g kW^{-1} hr^{-1}, as opposed to g/kg-fuel. For these cases we have converted the EF_{BC} (or EF_{EC}) values to g-BC/kg-fuel using either the reported measured specific fuel oil consumption (SFOC, kg-fuel kW^{-1} hr^{-1}) or EF_{CO2} (g-CO_2 kW^{-1} hr^{-1}), where

$$EF_{BC}\left(\frac{g\ BC}{kg\ fuel}\right) = \frac{EF_{BC}\left(\frac{g}{kW.hr}\right)}{SFOC\left(\frac{kg\ fuel}{kW.hr}\right)} \quad \text{(S1)}$$

or

$$EF_{BC}\left(\frac{g\ BC}{kg\ fuel}\right) = \frac{1000 \cdot EF_{BC}\left(\frac{g}{kW.hr}\right)}{EF_{CO2}\left(\frac{g\ CO_2}{kW.hr}\right)\left(\frac{12\ g\ C}{44\ g\ CO_2}\right)\left(\frac{1\ g\ fuel}{0.865\ g\ C}\right)\left(\frac{1\ kg}{1000\ g}\right)} \quad \text{(S2)}$$

where the 0.865 is the assumed mass fraction of carbon in the fuel. In cases where neither the SFOC or EF_{CO2} are directly reported, we have estimated the SFOC from the commonly used relationship

$$SFOC\left(\frac{g\ fuel}{kW.hr}\right) = \frac{c_0}{F_{load}} + c_1 \quad \text{(S3)}$$

where c_0 = 14.1205 and c_1 = 205.7169 and F_{load} is expressed as a fraction, not a percentage (Entec, 2002). This SFOC estimation method was necessary for only two studies, Sarvi et al. (2009) and Kasper et al. (2007).

3. The SP-AMS Collection Efficiency (CE)

The SP-AMS was calibrated during Calnex by determining the mass specific ionization efficiency (mIE_{BC}) for size-selected Regal black particles, based on the previously determined mobility/mass relationship for Regal black particles (Onasch et al., 2012). Atomized Regal black particles are collapsed into tightly packed agglomerates that are nearly spherical, and thus we expect good overlap between the sampled particle beam and the SP-AMS laser beam. The collection efficiency (*CE*) for sampled particles depends on the extent to which the sampled particle beam behaves similar to the Regal black calibration particles. If there is greater divergence of the particle beam, the *CE* will be less than unity because of lessened overlap between the particle beam and the SP-AMS laser beam. The two main issues that affect particle beam divergence in the aerodynamic lens are (i) particle shape and (ii) particle size. Nonspherical particles and smaller particles will cause greater particle beam divergence when sampled into vacuum due to lift forces and Brownian motion, respectively (Huffman et al., 2005;Liu et al., 1995a, b).

The measured SP_AMS rBC *CE* for on-road vehicle exhaust emissions in New York City, as determined in situ by comparing with an independent measurement for black carbon mass loading, was 0.11 (Massoli et al., 2012). In a separate study of on-road vehicle emissions in California by Dallmann et al. (In preparation), the SP-AMS rBC *CE* was measured to be 0.27. Based on these results we estimate the $CE_{BC,plume} = 0.2$, with an assumed uncertainty of ± 40%. For comparison, the campaign average *CE* was ~0.5 for non-plume ambient particles, determined by comparison of the SP-AMS to the SP2 (Massoli et al., In preparation), while a broader comparison of the SP-AMS with additional ship plume encounters is consistent with the smaller $CE_{BC,plume}$ used here (Buffaloe et al., In preparation). The ambient BC-containing particles were typically internally mixed with substantial amounts of non-BC material (Cappa et al., 2012), and therefore larger and more spherical than the plume BC particles and thus expected to exhibit a *CE* greater than the ship-plume *CE*.

The CE in the SP-AMS is not necessarily the same for the BC and the associated non-BC material (e.g. organics, sulfate) and will be, in general, larger for the non-BC material. The reason for this difference is that the BC containing (i.e., absorbing) particles that pass through the edges of the laser beam absorb less energy and heat less. The material that vaporizers first (i.e., under small increases in temperature) from the BC particles will always be the non-BC associated material, and this material may evaporate even if the BC material does not fully vaporize and get detected. This process is illustrated in the different laser power dependences for BC and associated non-BC materials reported in Onasch et al. (2012). Thus, we estimate that the *CE* for non-BC species in the plume, which determines the measurement accuracy, was $CE_{non\text{-}BC,plume} = 0.4 \pm 100\%$. The precision of the non-BC material measurements is expected to be substantially larger.

4. Measurements of Cloud Condensation Nuclei Emission Factors

The CCN instrument was operated such that it sampled sequentially in time at supersaturations (*SS*) of 0.3%, 0.4%, 0.5%, 0.6% and 0.7%, and then the cycle is repeated. The sampling time at each *SS* was 5 mins, with the exception of *SS* = 0.3% for which the sampling time was 10 mins to allow for stabilization after returning from *SS* = 0.7%. For some plumes (i.e. vessel speeds), the relative timing between the super saturation changes in the CCN counter and the the plume encounters allowed for determination of the EF_{CCN} at two *SS* values. To determine the EF_{CCN} for these plume subsets, the area ratio method was used (as described in the main text), but the area for both the CCN number concentration and $[CO_2]$ were calculated only for the period corresponding to operation at a given *SS*. To allow for determination of the CCN/CN ratio (i.e. the fraction of particles that act as CCN), EF_{CN} values were determined over periods corresponding to the appropriate *SS*.

5. SP2 Data Processing

The SP2 measures the incandescence emitted by refractory black carbon particles heated to their boiling point (~4000 K). The per particle rBC mass is proportional to the intensity of the emitted incandescence. The counting efficiency (i.e. detection efficiency) of the SP2 depends on (i) having the laser and particle beams properly aligned with respect to each other, (ii) the laser power and (iii) the particle size (Laborde et al., 2012b). It is this last aspect that is most relevant to the current study, in particular to the determination of the shape of rBC size distributions for small particles (<100 nm). Smaller particles have larger surface area-to-volume ratios (SA/V) than larger particles; this is exacerbated when particles are fractal like. For rBC particles to reach their boiling points and incandesce the rate of energy input by the laser must be greater than the

rate of energy loss from e.g. thermal conduction to the bath gas. For particles with volume equivalent diameters ($d_{p,VED}$) less than ~100 nm the heating may not be sufficient to bring the particle to a temperature that is high enough to lead to incandescence. In other words, cooling wins out and the particles do not incandesce. (For the SP-AMS, where the particle heating occurs in vacuum, this conductive cooling is not an issue and small particles that pass through the laser beam can be detected with equal efficiency to larger particles.) Whether an individual small rBC-containing particle will incandesce will depend, somewhat, on the shape of that particle. Thus, one should expect that, given a random population of rBC containing particles, the likelihood that a particle with $d_{p,VED} < \sim 100$ nm will give a measurable incandescence signal will be similarly random, but with a probability that decreases with $d_{p,VED}$. This has been observed previously (Schwarz et al., 2010;Laborde et al., 2012b), with the detection efficiency for the SP2 falling off precipitously below $d_{p,VED} \sim 100$ nm, with approximately a sigmoidal shape. This fall off in the detection efficiency (*DE*) was quantified after the CalNex campaign for this SP2 in the laboratory and was found to have a similar shape to literature observations (Schwarz et al., 2010;Laborde et al., 2012b). The specific fall off in *DE* with size used to correct the directly observed size distributions is shown in Fig. S1. The uncorrected size distributions used to generate Fig. 6 in the main text are shown for reference in Fig. S2. Ideally the *DE* for particles with $d_{p,VED} > \sim 100$ nm is unity (Laborde et al., 2012b). During CalNex, the *DE* for such particles was measured to be 0.7, which suggests a laser alignment problem. Further, the scattering traces (i.e. scattering intensity vs. time) for individual particles deviated from the ideal Gaussian shape (Gao et al., 2007;Moteki and Kondo, 2008), consistent with laser issues. Undoubtedly, the uncertainty in the *CE* correction for smaller particles is large given the steepness of the curve. However, we aim to use this correction in only a semi-quantitative manner to demonstrate (i) that

it is very likely that particle mode with $d_{p,VED} < 60$ nm exists and (ii) to provide a rationale for the lower EF_{BC} values derived from the SP2, compared to the other measurement techniques. It should be noted that the SP2 will always provide a lower bound on the rBC mass concentration because of the limited detection range and that non-symmetric uncertainties are appropriate. The positive uncertainty on the SP2 EF_{BC} is estimated for this study to be ~100%, based on results from Liggio et al. (2012) looking at relatively "fresh" emissions in a road-side environment. The negative uncertainty is estimated as 20%, based on consideration of how well fullerene soot represents ambient BC (Laborde et al., 2012a).

5. References

Agrawal, H., Malloy, Q. G. J., Welch, W. A., Wayne Miller, J., and Cocker III, D. R.: In-use gaseous and particulate matter emissions from a modern ocean going container vessel, Atmos. Environ., 42, 5504-5510, 2008a, doi:10.1016/j.atmosenv.2008.02.053.

Agrawal, H., Welch, W. A., Miller, J. W., and Cocker III, D. R.: Emission measurements from a crude oil tanker at sea, Environ. Sci. Technol., 42, 7098-7103, 2008b, doi:10.1021/es703102y.

Agrawal, H., Welch, W. A., Henningsen, S., Miller, J. W., and Cocker III, D. R.: Emissions from main propulsion engine on container ship at sea, J. Geophys. Res.-Atmos., 115, D23205, 2010, doi:10.1029/2009jd013346.

Cappa, C. D., Onasch, T. B., Massoli, P., Worsnop, D., Bates, T. S., Cross, E., Davidovits, P., Hakala, J., Hayden, K., Jobson, B. T., Kolesar, K. R., Lack, D. A., Lerner, B., Li, S. M., Mellon, D., Nuaanman, I., Olfert, J., Petaja, T., Quinn, P. K., Song, C., Subramanian, R., Williams, E. J., and Zaveri, R. A.: Radiative absorption enhancements due to the mixing state of atmospheric black carbon Science, 337, 1078-1081, 2012, doi:10.1126/science.1223447.

Entec, Quantification of emissions from ships associated with ship movements between ports in the European Community, Prepared for the European Commission.: http://ec.europa.eu/environment/air/pdf/chapter2_ship_emissions.pdf, access: 25 April 2011, 2002.

Gao, R. S., Schwarz, J. P., Kelly, K. K., Fahey, D. W., Watts, L. A., Thompson, T. L., Spackman, J. R., Slowik, J. G., Cross, E. S., Han, J. H., Davidovits, P., Onasch, T. B., and Worsnop, D. R.: A Novel Method for Estimating Light-Scattering Properties of Soot Aerosols Using a Modified Single-Particle Soot Photometer, Aerosol Science and Technology, 41, 125-135, 2007, doi:10.1080/02786820601118398.

Huffman, J. A., Jayne, J., Drewnick, F., Aiken, A. C., Onasch, T., and Worsnop, D.: Design, modeling, optimization and experimental tests of a particle beam width probe for the Aerodyne aerosol mass spectrometer, Aerosol Sci. Technol., 39, 1143-1163, 2005, doi:10.1080/02786820500423782.

Jayaram, V., Agrawal, H., Welch, W. A., Miller, J. W., and Cocker, D. R.: Real-Time Gaseous, PM and Ultrafine Particle Emissions from a Modern Marine Engine Operating on Biodiesel, Environ. Sci. Technol., 45, 2286–2292, 2011, doi:10.1021/es1026954.

Kasper, A., Aufdenblatten, S., Forss, A., Mohr, M., and Burtscher, H.: Particulate Emissions from a Low-Speed Marine Diesel Engine, Aerosol Science and Technology, 41, 24 - 32, 2007, doi:10.1080/02786820601055392.

Khan, M. Y., Giordano, M., Gutierrez, J., Welch, W. A., Asa-Awuku, A., Miller, J. W., and Cocker, D. R.: Benefits of two mitigation strategies for container vessels: cleaner engines and cleaner fuels, Environ. Sci. Technol., 46, 5049-5056, 2012a, doi:10.1021/es2043646.

Khan, M. Y., Russell, R. L., Welch, W. A., Cocker, D. R., and Ghosh, S.: Impact of Algae Biofuel on In-Use Gaseous and Particulate Emissions from a Marine Vessel, Energy & Fuels, 26, 6137-6143, 2012b, doi:10.1021/ef300935z.

Laborde, M., Mertes, P., Zieger, P., Dommen, J., Baltensperger, U., and Gysel, M.: Sensitivity of the Single Particle Soot Photometer to different black carbon types, Atmos. Meas. Tech., 5, 1031-1043, 2012a, doi:10.5194/amt-5-1031-2012.

Laborde, M., Schnaiter, M., Linke, C., Saathoff, H., Naumann, K. H., Möhler, O., Berlenz, S., Wagner, U., Taylor, J. W., Liu, D., Flynn, M., Allan, J. D., Coe, H., Heimerl, K., Dahlkötter, F., Weinzierl, B., Wollny, A. G., Zanatta, M., Cozic, J., Laj, P., Hitzenberger, R., Schwarz, J. P., and Gysel, M.: Single Particle Soot Photometer intercomparison at the AIDA chamber, Atmos. Meas. Tech., 5, 3077-3097, 2012b, doi:10.5194/amt-5-3077-2012.

Liggio, J., Gordon, M., Smallwood, G., Li, S.-M., Stroud, C., Staebler, R., Lu, G., Lee, P., Taylor, B., and Brook, J. R.: Are Emissions of Black Carbon from Gasoline Vehicles Underestimated? Insights from Near and On-Road Measurements, Environ. Sci. Technol., 46, 4819-4828, 2012, doi:10.1021/es2033845.

Liu, P., Ziemann, P. J., Kittelson, D. B., and McMurry, P. H.: Generating Particle Beams of Controlled Dimensions and Divergence: II. Experimental Evaluation of Particle Motion in Aerodynamic Lenses and Nozzle Expansions, Aerosol Science and Technology, 22, 314-324, 1995a, doi:10.1080/02786829408959749.

Liu, P., Ziemann, P. J., Kittelson, D. B., and McMurry, P. H.: Generating Particle Beams of Controlled Dimensions and Divergence: I. Theory of Particle Motion in Aerodynamic Lenses and Nozzle Expansions, Aerosol Science and Technology, 22, 293-313, 1995b, doi:10.1080/02786829408959748.

Massoli, P., Fortner, E. C., Canagaratna, M. R., Williams, L. R., Zhang, Q., Sun, Y., Schwab, J. J., Trimborn, A., Onasch, T. B., Demerjian, K. L., Kolb, C. E., Worsnop, D. R., and Jayne, J. T.:

Pollution Gradients and Chemical Characterization of Particulate Matter from Vehicular Traffic near Major Roadways: Results from the 2009 Queens College Air Quality Study in NYC, Aerosol Science and Technology, 46, 1201-1218, 2012, doi:10.1080/02786826.2012.701784.

Moteki, N., and Kondo, Y.: Method to measure time-dependent scattering cross sections of particles evaporating in a laser beam, J. Aerosol. Sci., 39, 348-364, 2008, doi:10.1016/j.jaerosci.2007.12.002.

Onasch, T. B., Trimborn, A. M., Fortner, E. C., Jayne, J. T., Kok, G. L., WilliamS, L. R., Davidovits, P., and Worsnop, D. R.: Soot Particle Aerosol Mass Spectrometer: Development, Validation and Initial Application, Aerosol Science and Technology, 46, 804-817, 2012, doi:10.1080/02786826.2012.663948.

Petzold, A., Weingartner, E., Hasselbach, I., Lauer, P., Kurok, C., and Fleischer, F.: Physical Properties, Chemical Composition, and Cloud Forming Potential of Particulate Emissions from a Marine Diesel Engine at Various Load Conditions, Environ. Sci. Technol., 44, 3800-3805, 2010, doi:10.1021/es903681z.

Petzold, A., Lauer, P., Fritsche, U., Hasselbach, J., Lichtenstern, M., Schlager, H., and Fleischer, F.: Operation of Marine Diesel Engines on Biogenic Fuels: Modification of Emissions and Resulting Climate Effects, Environ. Sci. Technol., 45, 10394-10400, 2011, doi:10.1021/es2021439.

Sarvi, A., Kilpinen, P., and Zevenhoven, R.: Emissions from large-scale medium-speed diesel engines: 3. Influence of direct water injection and common rail, Fuel Processing Technology, 90, 222-231, 2009, doi:10.1016/j.fuproc.2008.09.003.

Sarvi, A., and Zevenhoven, R.: Large-scale diesel engine emission control parameters, Energy, 35, 1139-1145, 2010, doi:10.1016/j.energy.2009.06.007.

Schwarz, J. P., Spackman, J. R., Gao, R. S., Perring, A. E., Cross, E., Onasch, T. B., Ahern, A., Wrobel, W., Davidovits, P., Olfert, J., Dubey, M. K., Mazzoleni, C., and Fahey, D. W.: The Detection Efficiency of the Single Particle Soot Photometer, Aerosol Science and Technology, 44, 612-628, 2010, doi:10.1080/02786826.2010.481298.

Table S1: Engine type, ship type and fuel type for the literature studies.

Study	Engine Type[^]	Vessel Name	Vessel Type	Build Year	Fuel Type(s)[+]
This study	MSD	R/V Miller Freeman	Research Vessel	1967	LSF
Khan et al. (2012a)	SSD	--	Container	--	HFO
Khan et al. (2012b)	MSD	T/S State of Michigan	Surveillance	1986	ULSD,Bio
Petzold et al. (2011)	MSD	n/a	n/a	--	HFO,MGO,Bio
Petzold et al. (2010)	MSD	n/a	n/a	--	HFO
Kasper et al. (2007)	SSD	n/a	n/a	--	HFO
Agrawal et al. (2008a)	SSD	--	PanaMax class container	1995	HFO
Agrawal et al. (2008b)	SSD	--	Suezmax class	--	HFO
Agrawal et al. (2008b)	MSD*	--	Suezmax class	--	MGO
Agrawal et al. (2010)	SSD	--	Post PanaMax class container	1998	HFO
Jayaram et al. (2011)	MSD	--	Harbor-craft	2007	MGO,Bio
Sarvi et al. (2009)	MSD	n/a	n/a	--	HFO/LSF
Sarvi et al. (2010)	MSD	n/a	n/a	--	HFO/LSF/??

[^] MSD = medium speed diesel; SSD = slow speed diesel
*Auxiliary Engine
[+] LSF = low sulfur fuel; HFO = heavy fuel oil; ULSD = ultra-low sulfur diesel; Bio = biofuel; MGO = marine gas oil
Cells with -- indicate information not reported in original study
n/a = not applicable

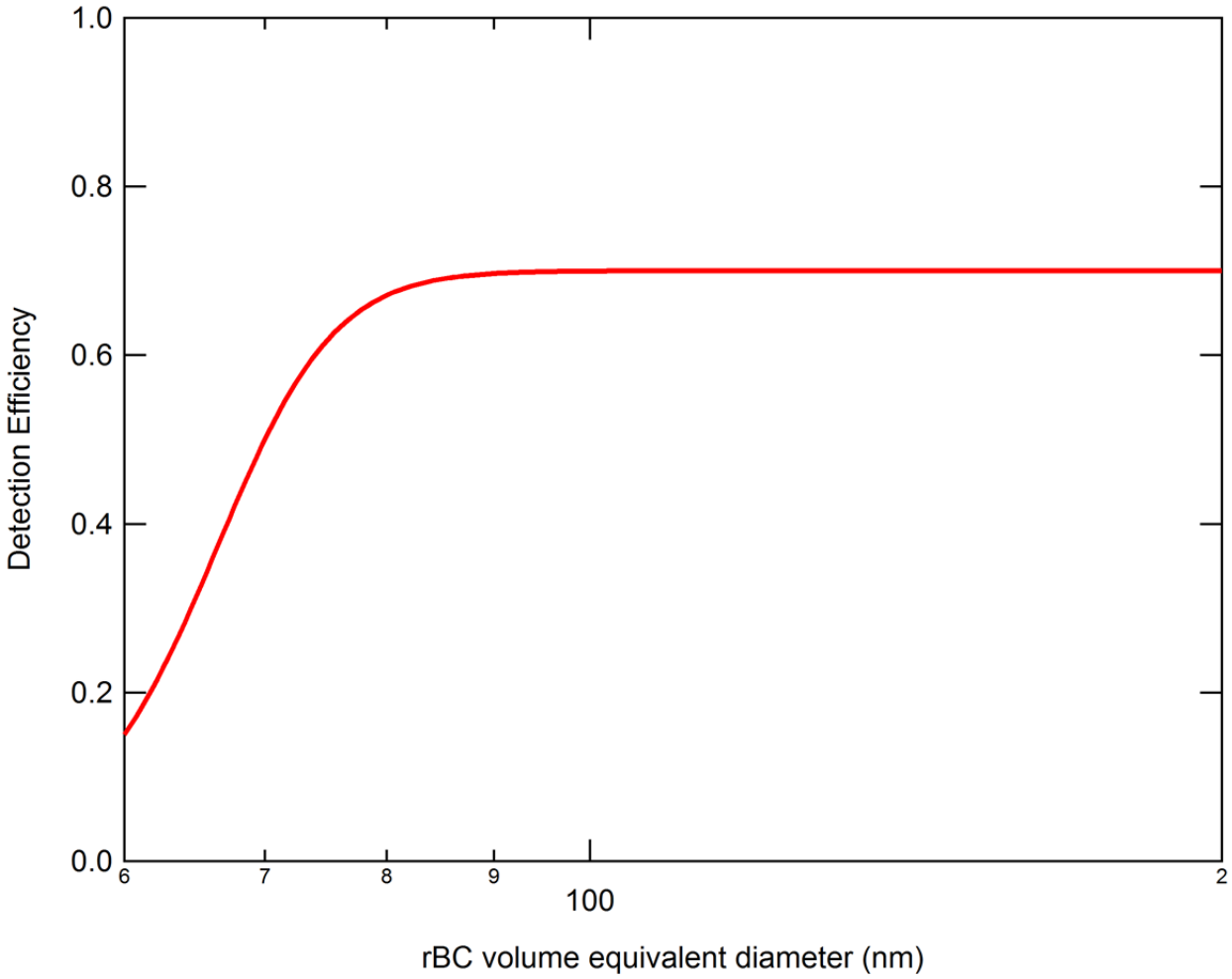

Figure S1. The detection efficiency for the SP2 used during CalNex as a function of size.

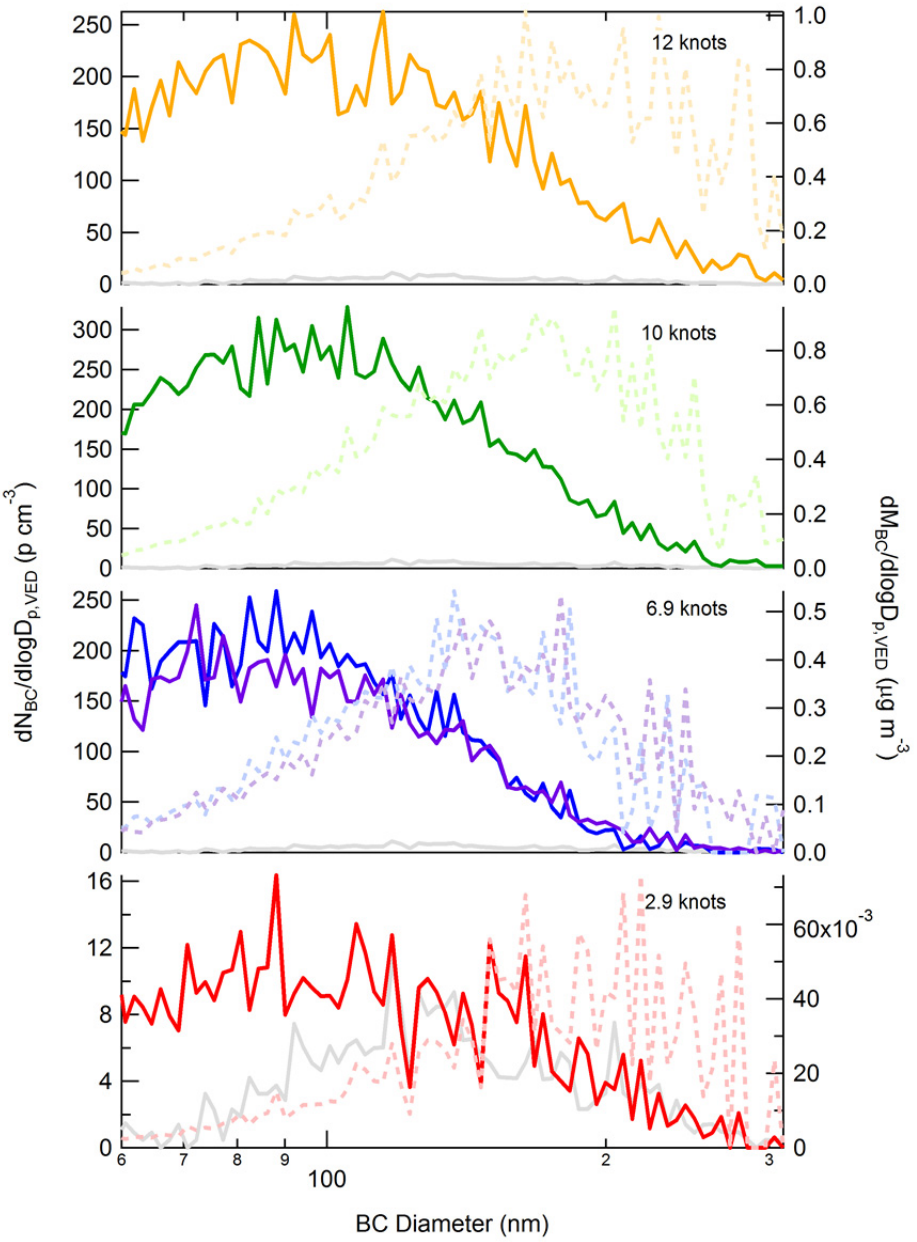

Figure S2. Number-weighted (left axis and solid lines) and mass weighted (right axis and dashed lines) size distributions for the rBC component of particles for each plume intercept, averaged over the entire plume. A size-independent detection efficiency of 0.7 has been applied. The number-weighted distributions for background (outside of plume) particles are shown as the grey traces in all panels. The speed of the R/V *Miller Freeman* corresponding to each plume is indicated on each panel.